Pergamon

Available online at www.sciencedirect.com
SCIENCE DIRECT®

Cement and Concrete Research 33 (2003) 1269–1276

CEMENT AND CONCRETE RESEARCH

# Hydration and properties of novel blended cements based on cement kiln dust and blast furnace slag

Maria S. Konsta-Gdoutos*,[1], Surendra P. Shah

*Center for ACBM, Department of Civil Engineering, Northwestern University, Evanston IL 60208, USA*

Received 20 February 2002; accepted 6 February 2003

**Abstract**

The aim of the present paper is to address the key technical issues pertaining to the utilization of cement kiln dust (CKD) as an activator for ground granulated blast furnace slag (GGBFS) to create nonconventional cementitious binders for concrete. The relatively high alkaline content of CKD is the predominant factor preventing its recycling in cement manufacture. However, it was observed that depending on the water-soluble alkali and sulfate compounds, CKD could provide the environment necessary to activate latent hydraulic materials such as GGBFS. Binary blends containing slag and CKDs from different sources were characterized and compared in terms of the rates of heat evolution and strength development, hydration products, and time of initial setting. A study of the effects of the influencing factors in terms of soluble alkali content, particle size, and free lime content was undertaken. The results confirm the dependence of the dissolution rate of slag on the alkalinity of the reacting system, and the importance of the optimum lime content on the rate of strength gain.


*Keywords:* X-ray diffraction; Hydration; Compressive strength; Cement kiln dust; GGBFS

## 1. Introduction

The environmental concerns related to Portland cement production, emission and disposal of cement kiln dust (CKD), is becoming progressively significant. CKD is a fine-grained, particulate material readily entrained in the combustion gases moving through the kiln. It is composed primarily of variable mixtures of calcined and uncalcined feed materials, fine cement clinker, fuel combustion by-products, and condensed alkali compounds [1]. The generation of CKD is responsible for a significant financial loss to the cement industry in terms of the value of raw materials, processing, energy usage, and dust collection and disposal. Cement manufacturing plants generate approximately 30 million tons of CKD worldwide per year [2]. The U.S. cement industry generates about 4.1 million tons of CKD every year, 3.3 million tons of which is landfilled and only 0.75 million tons enter commerce as by-products [3].

The relatively high alkaline content of CKD is the predominant factor preventing its recycling in cement manufacturing. All CKDs frequently contain alkalis ($Na_2O$, $K_2O$) and sulfates in much higher percentages than those in Portland cement. CKD often contains a large amount of free lime, thus making it a substitute for fertilizers and lime in stabilizing wastewater streams. Furthermore, studies have shown that CKD can be effectively used in soil and sludge stabilization. It has also been successfully used as inorganic filler in bituminous paving and asphaltic roofing [4].

Because the characteristics of CKD vary from plant to plant, only a small amount of CKD (< 15% cement replacement) is used in the cement and concrete industry. However, its high alkali and sulfate content makes it an excellent activator for pozzolanic materials. The dissolution rate of materials with latent pozzolanic properties such as blast furnace slag generally depends on the alkali concentration of the reacting system [5]. Latent hydraulic materials develop pozzolanic activity and act as hydraulic cements once their glass network disintegrates when attacked by $OH^-$ ions. The solubilities of Si, Ca, Al, and Mg are functions of the pH. At a pH lower than 11.5, the equilib-

* Corresponding author. Department of Civil Engineering, Democritus University of Thrace, GR-671 00 Xanthi, Greece. Tel.: +30-25410-79658; fax: +30-25410-25435.

*E-mail address:* mkonsta@civil.duth.gr (M.S. Konsta-Gdoutos).

[1] On sabbatical leave from the Department of Civil Engineering, Democritus University of Thrace, GR-671 00 Xanthi, Greece.

0008-8846/03/$ – see front matter © 2003 Elsevier Science Ltd. All rights reserved.
doi:10.1016/S0008-8846(03)00061-9

rium solubility of silica is low and slag does not dissolve. As a result, more $Ca^{+2}$ and $Mg^{+2}$ enter into the solution and an impermeable aluminosilicate coating covers the surfaces of the slag grains, which inhibits further hydration [6]. A chemical activator is required for further hydration of slag. Activators generally include all alkali hydroxides and salts, with the least soluble salts being the most effective [7,8]. Because all salts are neutral solutions they exhibit only a weak activating effect; however, when they are combined with lime they undergo an exchange reaction with $Ca^{+2}$ and hydroxide ions. Solutions of sodium or potassium hydroxides are then formed, which attack and disintegrate the aluminosilicate glass. The presence of sulfate ions, supplied either by gypsum or alkali sulfates, accelerates the dissolution of slag by reducing the concentrations of $Ca^{+2}$ and $Al^{+3}$ in the mix to form ettringite.

Limited information on the pertinence of CKD as an activator for pozzolanic materials is available. Sprouse [9] applied and received a patent for a cement that combined ground blast furnace slag with CKD. Amin et al. [10] studied the effect of kiln dust content and the calcination temperature on the hydration of granulated slag. Hydration products such as CSH, $C_4AH_{13}$, $C_2AH_X$, $Ca(OH)_2$, hydrogarnet, and calcite were identified using the DTA technique. Their results indicated that the crystallinity and the content of the cementitious phases, especially $\beta$-$C_2S$, increased with calcination temperature. They concluded that activation of slags increases with increasing the content and the calcination temperature of the CKD. El-Didamony et al. [11] evaluated the effect of washed and calcined kiln dust with anhydrite. They found that the activation of the slag increases with firing temperature of the kiln dust and the amount of added anhydrite. Kiln dust calcined at 1300 °C with 15% anhydrite was found to be suitable for the production of supersulfated cement. Recently, the production of active $\beta$-$C_2S$, $C_{12}A_7$ and $C_2AS$ cements using different proportions of a low-CaO fly ash and a lime-rich CKD as raw materials was proposed [12].

The objective of the present work is to understand the interaction of CKD with slag in order to explore the feasibility and the approaches to development of a new generation of more durable CKD-activated slag blends. Ground granulated blast furnace slag (GGBFS) has successfully been used with Portland cement to produce high-performance cement blends that are more economical and environmentally friendly. The use and effectiveness of CKD as an activator for slag depends upon its physical and chemical characteristics, most importantly, the alkali and free lime content, and the amount of carbonates and sulfates. The effectiveness of the alkali activation of slag will depend on the alkalinity provided by the CKD. It is expected that the high free lime content of the CKD will improve the hydration process by accelerating hydration and forming more crystalline products of hydration. Sulfate ions provided either by alkali salts or anhydrite will expedite the hydration process and accelerate the pozzolanic reaction through the formation of ettringite. The experimental approach in this work includes the characterization of binary blends containing 50% slag and 50% CKD in terms of the rates of heat evolution and strength development, hydration products, and time of initial setting. A study of the effects of the influencing factors of four different CKDs in terms of soluble alkali content, particle size, and free lime content was undertaken. The results indicate the dependence of the dissolution rate of slag on the alkalinity of the system and the importance of the optimum lime content on the rate of strength development.

## 2. Materials

Four different types of CKDs and a granulated blast furnace slag were selected for this study. The chemical composition and physical properties of the materials are given in Table 1. Compositions of the individual components were determined by X-ray fluorescence (XRF) spectroscopy. The slag meets the classification requirements of ASTM C 989 for Grade 100. The specific gravity is 2.90 and the Blaine specific surface is 4460 $cm^2/g$. Results from X-ray diffraction (XRD) analysis (Fig. 1) indicated that the slag consisted mainly of a glassy phase. The small sharp peaks are due to traces of crystalline phases of merwinite ($C_3MS_2$) and akermanite ($C_2MS_2$).

Results from the XRD analysis of the four CKD samples are shown in Fig. 2. Calcite ($CaCO_3$) was identified as the prevailing phase for all four samples. The CKD samples, identified as E, P, A, and X, were representative of various plant operating conditions affecting dust composition and reactivity, such as the feed raw materials, kiln type, and dust-collection systems. CKDs (E) and (P) were generated from wet process kilns and were collected by electrostatic precipitators and baghouses, respectively. They contained large amounts of calcite, expressed as high LOI, and small

Table 1
Results of oxide analyses of CKD and GGBFS by XRF

| Compound (wt.%) | CKD (E) | CKD (P) | CKD (A) | CKD (X) | GGBS Gr 100 |
|---|---|---|---|---|---|
| $SiO_2$ | 14.67 | 15.7 | 11.5 | 8.96 | 31.96 |
| $Al_2O_3$ | 5.06 | 5.061 | 4.68 | 2.667 | 10.31 |
| $Fe_2O_3$ | 3.46 | 2.58 | 2.04 | 2.21 | 1.42 |
| CaO | 56.99 | 45.5 | 50.2 | 48.6 | 45.98 |
| MgO | 1.04 | 2.33 | 1.34 | 3.141 | 7.02 |
| $SO_3$ | 8.45 | 5.68 | 16.7 | 7.23 | 2.13 |
| $K_2O$ | 6.073 | 5.33 | 5.86 | 6.81 | 0.31 |
| $Na_2O$ | 0.6 | 0.89 | 1.015 | 0.54 | 0.26 |
| Alkali equivalent | 4.60 | 4.40 | 4.871 | 5.021 | 0.38 |
| Water-soluble alkali equivalent[a] | 2.25 | 1.69 | 2.59 | 3.30 | NA |
| $P_2O_5$ | 0.102 | 0.077 | 0.085 | – | 0.02 |
| $Cl^-$ | 0.532 | 1.802 | 0.732 | 1.4 | – |
| fCaO | 8 | 5.1 | 13.9 | 26.9 | |
| LOI | 15.10 | 25.5 | 9.56 | 17.92 | 0.2 |

[a] Measured by atomic absorption.

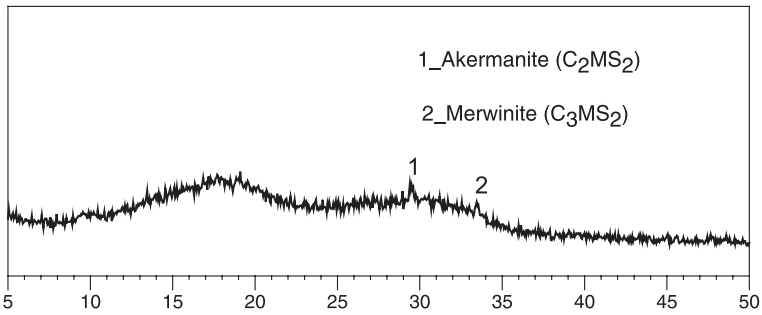


Fig. 1. XRD of the GGBFS used.

amounts of free lime. CKDs exhibiting high levels of carbonation and lacking free lime are usually stockpiled and considered less reactive, since the calcite is essentially nonreactive. CKD (P) also contained traces of dolomite [$CaMg(CO_3)_2$]. Dolomitic dusts are characterized by higher MgO contents, which are usually considered more slowly reactive.

CKD (X) is also a dolomitic dust obtained from a dry process kiln with a precalciner and a preheater, and collected by a baghouse. CKD (A) was removed from a long dry kiln with electrostatic precipitators. Both CKDs contained small amounts of calcite and high amounts of free lime indicating that more $Ca^{+2}$ will be available for a pozzolanic reaction. CKD (A) contained significant amounts of anhydrite. Traces of portlandite were identified in CKD (X) implying that the CKD has been exposed to moisture. Alkali sulfate salts were present in all four CKDs. Aphtithalite [$K_3Na(SO_4)_2$] was identified in CKDs (X) and (E), while CKD (E) and (A) contained arcanite ($K_2SO_4$). CKDs (P), (A), and (X) also contained sylvite (KCl).

An important physical characteristic of the CKDs is their particle size, which is shown in Fig. 3. The finest material used is CKD (A) with a specific surface of 8270 $cm^2/g$ and a mean equivalent spherical particle diameter of 9 μm. CKD (A) is also the most uniform: 57% fall into the narrow range of 1–10 μm and 93% are smaller than 45 μm. CKD (E) is the coarsest one with a mean diameter of 60 μm and is evenly divided between 45 and 100 μm. In CKDs (P) and (X), 75% of their particles are in the range between 1 and 45 μm. They both have a very similar particle size distribution, with a mean particle size of approximately 18 μm, and specific surfaces of 5410 and 6140 $cm^2/g$, respectively.

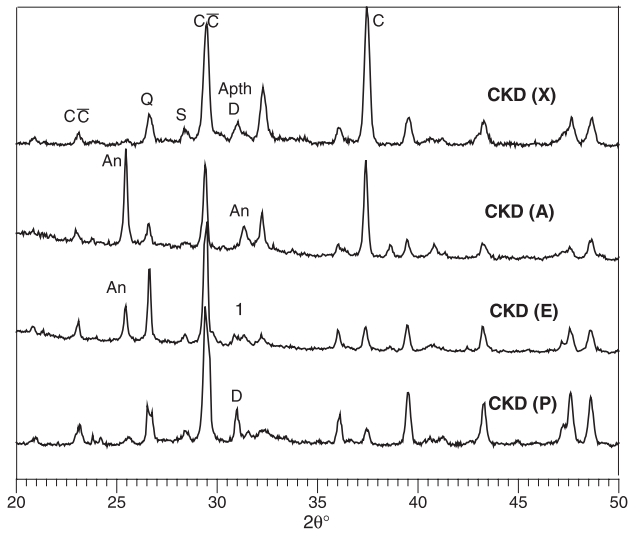


Fig. 2. XRD of the four raw cement kiln dusts P, E, A, and X. CC = calcite, C = lime, D = dolomite, Q = quartz, An = anhydrite, 1 = alkali salts (apthitalite, arcanite), S = sylvite.

## 3. Experimental program

### 3.1. Heat of hydration

The heat of hydration of CKD–slag pastes was measured using an adiabatic DSS Qdrum calorimeter. Blended material and deionized water were mixed according to ASTM C 305 using a Hobart mixer. After mixing, the paste was cast in a $2 \times 4$ in. ($50 \times 100$ mm) plastic cylinder mold. A temperature probe inserted into the cylinder recorded the adiabatic heat of hydration for 72 h. The time of initial setting of the CKD–slag pastes was determined using a Vicat apparatus according to ASTM C191.

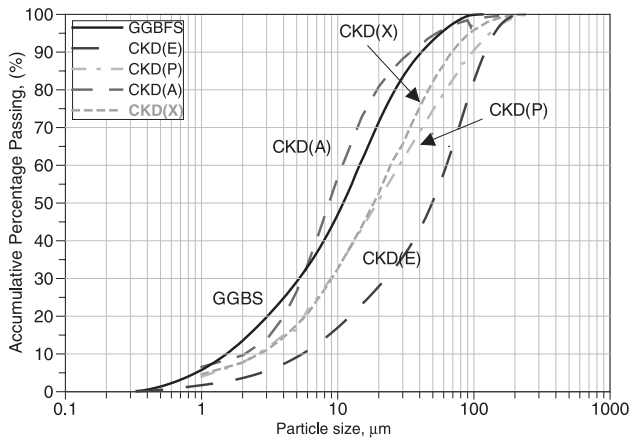


Fig. 3. Particle size distribution of the materials used.

### 3.2. Compressive strength

The compressive strength of cylindrical mortar specimens of 3 × 6 in. (75 × 150 mm) was determined according to the ASTM C 39-94 at 7, 28, and 56 days, and was calculated as the average of three specimens with consistent results. Mortars were mixed in accordance with EN 196-1:1987 with 450 g of binder blend, 1350 g of natural sand, and 225 g of water. After demoulding, specimens were cured on shelves in a moist curing room until testing. All test specimens were capped with a high-sulfur capping compound before testing, according to ASTM C 617.

### 3.3. X-ray diffraction

XRD was employed to identify the phases present in hydration products, using standard monochromatic CuKα radiation and operating at 40 kV and 20 mA. Scanning was performed at 0.05° 2θ step size, at 2 s per step, between 5 and 50°. Samples were prepared by crushing paste specimens into fine powder. To stop hydration at the desired ages, the crushed materials were slurried with 200-proof ethanol. The powder was vacuum filtered, air-dried, and reground before mounting in the XRD sample holders.

## 4. Results and discussion

### 4.1. Time of setting

The time at which the needle penetrates 25 mm into the pastes at room temperature was taken to define the initial setting, following ASTM 191. The time of initial setting for all blends is shown in Fig. 4. OPC reached initial set in 4.5 h, whereas for the OPC–slag blend an increase was observed and, as expected, time of setting was extended for 50 min. Time of setting was much shorter than the control blends for the blend with CKD (A), which may be due to the formation of ettringite; CKD (A) contains a very high amount of sulfate (≈17%). Significant retardation was observed for the slag blends activated with CKDs (E), (P), and (X). Initial setting time for the blends with CKD (P) and (X) were very similar, around 7 h and 30 min for the CKD (P)–slag blend, and almost 9 h for the blend with CKD (X). Slag activated with CKD (E) took more than 14 h to reach the initial set, which coincides with the end of the dormant period and the beginning of the acceleration period of the rate of heat evolution curve. However, a gradual stiffening of the paste and a change in rigidity was observed after the first 5 h of curing for all three blends activated with CKD (E), (P), and (X), which is believed to be caused by the formation of AFm phases throughout the fresh paste.

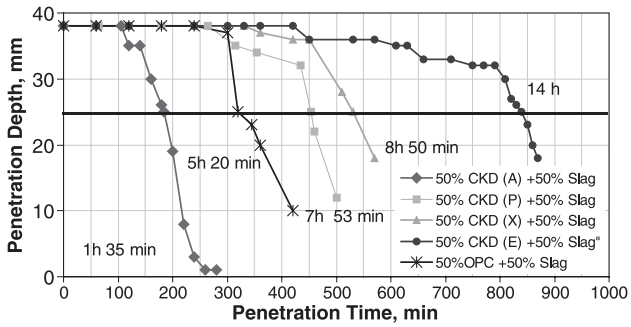


Fig. 4. Comparison of the time of initial set between the slag blends activated with CKDs A, P, E, and X and the control OPC–slag blend.

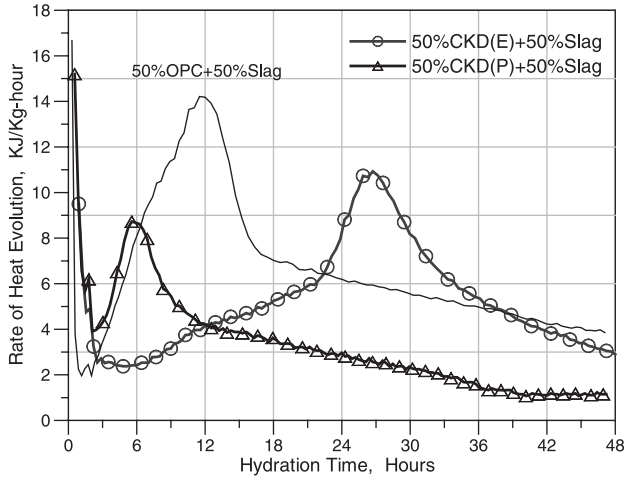


Fig. 5. Rate of heat evolution of the slag mixes activated with 50% CKD (E) and 50% CKD (P) compared to typical OPC–slag blends.

### 4.2. Heat of hydration

The heat evolution curves of the slag activated in mixes with 50% CKD (E) and CKD (P) are presented in Fig. 5. It can be seen that the trend of heat evolution of both blends is similar to that of the Portland cement–slag blend. One initial peak appears before the induction period, which is attributed to the rapid dissolution of alkali sulfates and aluminates. One lower peak also appears after the induction period for both blends, indicating a lower degree of slag activation.

The slag blend activated with CKD (E) was characterized by a very long induction period of approximately 18 h, which also corresponded to a very long delay in setting time. An increase in the time at which the maximum rate of heat development occurs has already been observed in ternary OPC–CKD (E)–slag mixes in previous work [13,14]. During the early period of reaction, gypsum and alkali sulfates dissolve and react at the surfaces of the aluminate and ferrite phases. In the presence of sufficient amounts of $Ca^{+2}$ and $SO_4^{2-}$ in the liquid phase of the mix, ettringite is formed and the dissolution of slag is greatly accelerated. It appears that the dissolution process of slag activated with CKD (E) is initially much slower, as the result of the slow rate of supply of $K^+$ and $SO_4^{2-}$. This can be attributed to the precipitation of syngenite, $K_2Ca(SO_4)_2$,

due to the high potassium content of the kiln dust, which also explains the stiffening observed during the long setting period. Nevertheless, a much higher accelerated peak appeared later indicating a higher degree of activation and possibly a higher rate of strength development.

Heat evolution curves of blends activated with CKDs (A) and (X) are shown in Fig. 6. Both blends gave two peaks before the dormant period and one accelerated but a very diffused peak after the dormant period. The very strong initial peak, which appears before the dormant period, is attributed to the combined effect of the hydration of high free lime content and the dissolution of alkali sulfates. The dormant period appears very short, indicating a vigorous dissolution of ions and an accelerated initial formation of hydration products. The rate of deceleration period is higher for the blend with CKD (A) indicating a more intense and more continuous formation of hydration products when compared to both the OPC–slag blend and the CKD (X)–slag blend.

### 4.3. X-ray diffraction

XRD was used to identify the phases formed during hydration. Fig. 7 shows the XRD pattern corresponding to slag activated with CKD (P), up to 28 days of hydration. C-S-H hydration products are known to produce broad diffusion peaks at approximately 29° 2θ; however, XRD patterns in this region overlap with the major peak for calcite at 29.4° 2θ. This characteristic peak of the calcite dominates the diffractogram at all ages. Calcite peaks remain constant indicating that carbonate particles are inert and do not participate in any hydration reaction releasing $Ca^{+2}$. The reactivity of the CKD is a function of the alkali and free lime content. The chemical and mineralogical analysis of CKD (P) (Fig. 2) showed the presence of negligible amounts of free lime and excessive amounts of carbonates, which is indicative of the limited availability of

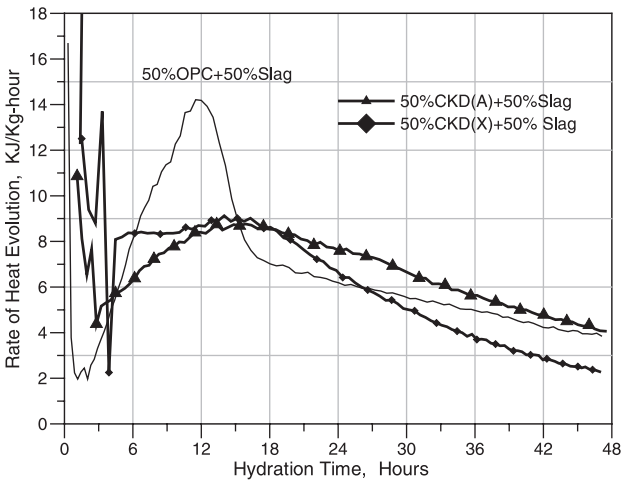


Fig. 6. Rate of heat evolution of the slag mixes activated with 50% CKD (A) and 50% CKD (X) compared to typical OPC–slag blends.

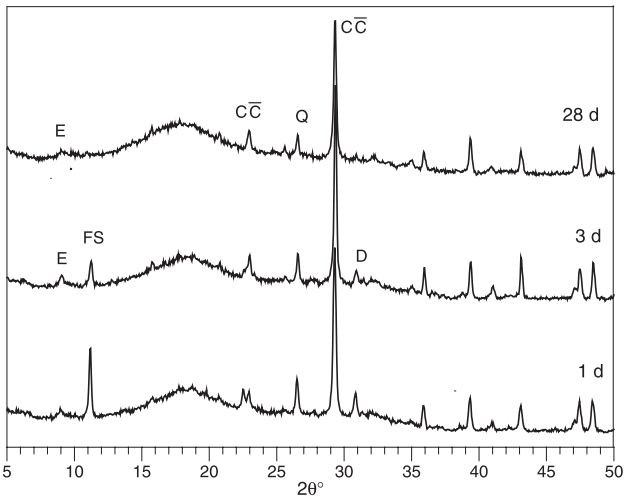


Fig. 7. XRD pattern of the CKD (P)–slag paste hydrated for 1, 3, and 28 days. CC = calcite, D = dolomite, Q = quartz, E = ettringite, FS = Friedel's salt.

$Ca^{2+}$. At 1 day, hydration products were ettringite and an AFm phase. Ettringite is a stable hydration product only while there is a sufficient supply of sulfates. When the sulfate source is not able to readily supply enough sulfate ions before the alumina content has completely hydrated, ettringite is converted to monosulphoaluminate. In place of sulfates, other ions such as chloride ions can appear and these phases are known as AFm phases. The AFm phase identified in this blend is the calcium monochloroaluminate hydrate, also known as Friedel's salt, which is the result of the high chloride content (1.8%) of the CKD (P). From 1 to 3 days of hydration, the ettringite and the Friedel's salt coexist. At this time, a decrease of the Friedel's salt peak occurs due to the presence of sulfate ions. Further, a decrease in the amount of dolomite (2θ = 30.94°, 41.43°) was observed at 3 days, although no products associated with the dedolomization reaction were detected. It should be noted that it was not possible to identify any $Ca(OH)_2$ peaks up to 28 days of hydration.

Fig. 8 shows the XRD pattern for the slag activated with CKD (E). This blend unexpectedly exhibited a very long setting time. A more detailed examination of the diffractogram at 6 h of hydration revealed the existence of syngenite peaks, $K_2Ca(SO_4)_2$, at 2θ = 31.3°, 28.2°. The precipitation of syngenite occurred due to the high potassium content of the dust, resulting in the removal of sulfate and potassium ions from the pore solution. The peaks were no longer detectable after 24 h of hydration. The subsequent release of sufficient sulfate ions from the dissolution of syngenite and the favorable ratio of $SO_4^{-2}$ to $Al(OH)_4^-$ caused the formation of well-crystallized ettringite, which persisted up to 7 days of hydration. Some calcium aluminate hydrates were also detected. No $Ca(OH)_2$ could be detected after 7 days of hydration indicating that the available lime was all consumed.

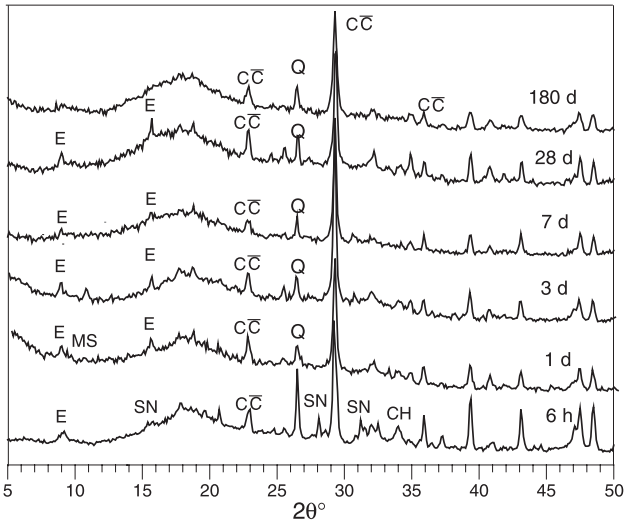


Fig. 8. XRD pattern of the CKD (E)–slag paste hydrated for 1, 3, 7, 28, and 180 days. CC = calcite, Q = quartz, E = ettringite, MS = monosulfoaluminate, CH = $Ca(OH)_2$, SN = syngenite.

The diffractogram of the blend with CKD (A) is shown in Fig. 9. At 6 h of hydration, the formation of gypsum due to the rehydration of the anhydrite was observed. Gypsum was consumed rapidly and was no longer detectable after 6 h of hydration. Ettringite was formed within the first hour of mixing and by 3 h was responsible for the very short setting time of the mix. Ettringite and $Ca(OH)_2$ remained the principal matrix phases up to 28 days of hydration. For this type of blend, slag was essentially activated with calcium sulfate such as in the case of supersulfated cement.

Fig. 10 shows the XRD pattern corresponding to slag activated with CKD (X). At early hydration, the evolution of the peaks of ettringite and monosulfoaluminate (2θ = 9.85°) is shown. The Friedel's salt formation is quite evident at 1 day of hydration. Its peak increases up to 3 days, then it decreases and a small amount may be detected at 7 days. A further release of aluminum from the decomposition of Friedel's salt causes the formation of ettringite. Its peaks increase again at 7 days and small amounts of monosulfoaluminate appear up to 28 days of hydration. Both phases are very stable and, as in Portland cement pastes, can coexist. Unreacted $Ca(OH)_2$ can be detected in the mix even after 28 days. As in the case of the other dolomitic dust CKD (P), a decrease in the amount of dolomite (2θ = 30.94°, 41.43°) was observed after 7 days.

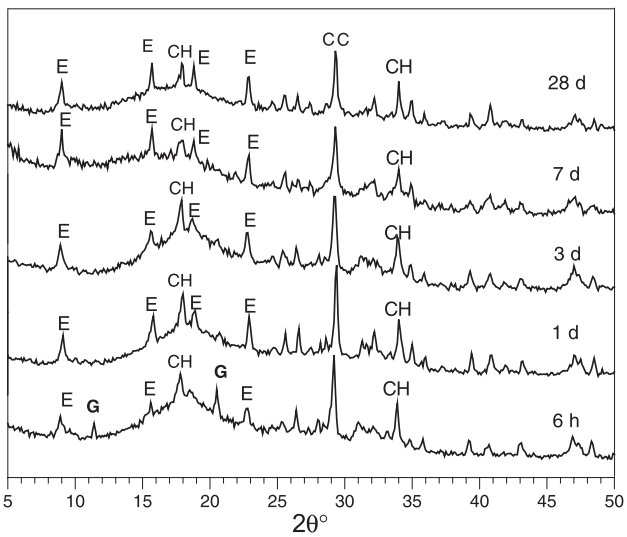


Fig. 9. XRD pattern of the CKD (A)–slag paste hydrated for 6 h, 1, 3, 7, and 28 days. CC = calcite, Q = quartz, E = ettringite, MS = monosulfoaluminate, CH = $Ca(OH)_2$, G = gypsum.

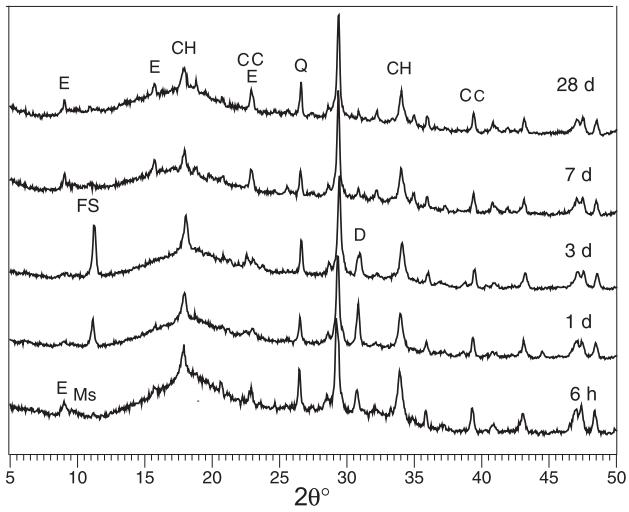


Fig. 10. XRD pattern of the CKD (X)–slag paste hydrated for 6 h, 1, 3, 7, and 28 days. CC = calcite, Q = quartz, D = dolomite, E = ettringite, MS = monosulfoaluminate, CH = $Ca(OH)_2$, FS = Friedel's salt.

### 4.4. Compressive strength

The development of compressive strength for the CKD–slag blends up to 56 days is shown in Fig. 11. Typical results

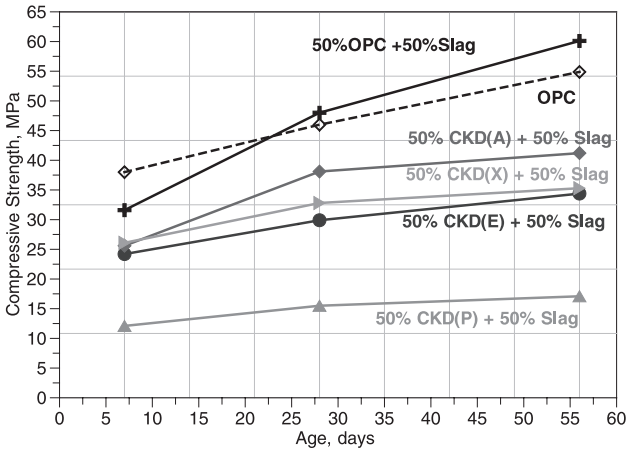


Fig. 11. Rate of compressive strength development of slag mortar blends activated with CKDs P, E, A, and X, compared with OPC and OPC–slag blends.

were obtained for the two reference blends. When compared to Portland cement concrete, use of Grade 100 slag typically results in lower compressive strengths at early ages, but equal or higher at later ages [15]. At the age of 7 days, the compressive strength of the cement–slag blend was lower than that of the OPC concrete. However, both the 28- and 56-day compressive strength was the highest of all blends, indicating a high degree of pozzolanic reaction.

Compressive strength of all four CKD–slag blends increased with curing time indicating slag activation by the CKD and the formation, precipitation, and accumulation of calcium silicate hydrates as products of hydration. Strength of all CKD–slag blends was always lower compared to OPC and OPC–slag mixes, at all ages. Our earlier study has also shown that CKD–slag blends developed a higher porosity when compared to the control OPC–slag blend, which may result in lower strength development [16]. The slag blend activated with CKD (P) had the lowest early and late strength of all the mixtures, ranging from 12.1 MPa at 7 days to 17.2 MPa at 56 days. CKD (P) lacks adequate quantities of lime for a pozzolanic reaction, and its water-soluble $Na_2O$ equivalent content (1.69%) is much lower than the optimum quantity of 3% by mass of slag, as defined by most researchers. Therefore, it is reasonable to assume that the activation of slag with CKD (P) is more the case of a weak effect of alkali activation, and that without the optimum supply of $Ca(OH)_2$ the pozzolanic reaction cannot be sustained. For this blend, CKD (P) acts mostly like a relatively inert diluent, with its fine particles acting as fillers, and possibly serves as crystallization nuclei.

Slag blends activated with CKDs (A), (E), and (X) had almost the same 7-day strength of approximately 25 MPa, indicating a high degree of slag activation. After 56 days of hydration, the compressive strength of the three slag blends with CKDs (E), (A), and (X) ranged from 34.4 to 41.2 MPa, with the highest strength achieved by the blend activated by CKD (A), followed by the two slag blends with CKD (E) and (X). The combination of both chemical and physical characteristics is critical to the strength performance. The fine and uniform size distribution of the CKD (A) provided a higher specific surface and promoted a more intense reaction. Slag blends activated with CKDs (E) and (X) showed similar strength gain. The lower rate of strength development of the blend with CKD (X) at later ages, when compared with CKD (E), may be attributed to the more than optimum amount of $Ca(OH)_2$ for the pozzolanic reaction. The remaining unreacted $Ca(OH)_2$ weakens the hardened matrix. This is in agreement with the results of Shi [17] from studies in lime–pozzolan cements. Another possible explanation could be the volume instability and unsoundness of the matrix, introduced by the dedolomization reaction of the CKD (X). Comprehensive studies, including NMR spectroscopy and SEM study of the microstructure, are required to further characterize the composition of the hydration products.

## 5. Conclusions

The engineering properties of the selected CKD–slag mixes developed in this study provide evidence that secondary materials such as CKD can be successfully utilized to activate blast furnace slag. Kiln dust–slag concrete, with good overall performance regarding setting time, temperature rise, and mechanical properties, can be produced with CKDs covering a wide range of chemical composition and fineness, and can essentially be regarded as a future alternative material to OPC. With appropriate proportioning and mix design, the optimum amount of the CKD can be determined for ultimate performance. The following conclusions are based on the experimental results presented in this paper:

1. The combination of both chemical and physical characteristics of CKD is critical in controlling the mechanisms of activation of GGBFS, the properties of the hydration products, and the rate of strength development. Adequate initial alkali concentration and the presence of sulfates have a decisive influence on slag activation and initial hydration. Further hydration and the formation of hydration products, leading to higher rate of strength development, are determined by the availability of $Ca^{+2}$ provided by the free lime content of the CKD.

2. Compressive strength of all four CKD–slag blends increased with curing time, indicating slag activation by the CKD and the formation, precipitation, and accumulation of products of hydration, similar to the ones found in typical OPC and OPC–slag systems. The main phases present in hardened pastes of CKD–slag blends have been determined. The variation of the chemical composition of the CKDs results in the formation of different hydration products at early hydration ages. At later ages, C-S-H gel and the stable sulfoaluminate hydrate ettringite are the major hydration products for all the CKD–slag blends. In the cases where the free lime content of the CKD exceeds the requirements for the pozzolanic reaction, the remaining unreacted crystalline $Ca(OH)_2$ may show a slight decrease on the strength development and possibly affect some durability properties. Further testing is under way at the center of ACBM at Northwestern University to elucidate durability aspects.

3. The calcium carbonate particles of the CKDs are essentially inert and do not participate in the hydration reaction. CKDs with water-soluble alkali content higher than 2% $Na_2O$ equivalent, low levels of carbonates, and free lime contents greater than 5% per mass of slag are considered more reactive and result in blends with higher strength developments.

4. When potassium concentrations in the pore solution are high and the $SO_4^{2-}$ are supplied very quickly, the precipitation of syngenite, $K_2Ca(SO_4)_2$, may occur, resulting in the removal of sulfate and potassium ions from the pore solution. The decrease of the alkali concentration of the pore solution reduces the pH and retards the slag dissolution and hydration.

5. The volume stability of any CKD–slag blend using a dolomitic kiln dust remains an area that requires further research.

## Acknowledgements

The present research was carried out at the Center for Advanced Cement-Based Materials (ACBM), Northwestern University. The authors acknowledge the ACBM center and the National Science Foundation (CMS-0086819) for their support.

## References

[1] ASTM D 5050-90, Standard guide for commercial use of lime kiln dusts and portland cement kiln dusts, Annual Book of ASTM Standards, vol. 04.01, ASTM, Philadelphia, PA, 1990, pp. 109–110.
[2] T.D. Dyer, J.E. Halliday, R.K. Dhir, An investigation of the hydration chemistry of ternary blends containing cement kiln dust, J. Mater. Sci. 34 (20) (1999 Oct.) 4975–4983.
[3] J.I. Bhatty, Alternative Uses of Cement Kiln Dust, RP327, Portland Cement Association, Skokie, IL, 1995.
[4] R.J. Collins, J.J. Emery, Kiln dust–fly ash systems for highway bases and subbases, Report No. FHWA/RD-82/167, USDOE and USDOT, Washington, DC, September 1983.
[5] S.-D. Wang, X.C. Pu, K.L. Scrivener, P.L. Pratt, Alkali activated slag cement and concrete: a review of properties and problems, Adv. Cem. Res. 7 (27) (1995) 93–102.
[6] S. Song, H.M. Jennings, Pore solution chemistry of alkali-activated ground granulated blast-furnace slag, Cem. Concr. Res. 29 (2) (1999) 159–170.
[7] C. Shi, R. Day, A calorimetric study of early hydration of alkali–slag cements, Cem. Con. Res. 29 (6) (1995) 1333–1346.
[8] B. Talling, J. Brandstetr, Clinker-free concrete based on alkali activated slag, in: S.L. Sarkar, S.N. Ghosh (Eds.), Mineral Admixtures in Cement and Concrete, ABI Books, India, 1993, pp. 296–341.
[9] J.H. Sprouse, Cements, mortars, and concretes, United States Patent #4451295, 1984.
[10] A.M. Amin, E-Ebied, H. El-Didamony, Activation of granulated slag with calcined cement kiln dust, Silic. Ind. 60 (3–4) (1995) 109–115.
[11] H. El-Didamony, A.H. Aly, A.M. Sharara, A.M. Amin, Assessment of cement dust with anhydrite as an activator for granulated slag, Silic. Ind. (1–2) (1997) 31–35.
[12] A. Xu, S.L. Sarkar, Active $\beta$-$C_2S$ cement from fly ash and kiln dust. Fly ash, silica fume, slag, and natural pozzolans in concrete, Proceedings of Fifth International Conference, American Concrete Institute, Detroit, SP 153-12, 1995, pp. 213–227.
[13] K. Wang, M.S. Konsta-Gdoutos, P.M. Babaian, S.P. Shah, Study of cement kiln dust–slag blended cement for durable concrete, International Symposium on High Performance Concrete: Workability, Strength and Durability, Hong Kong and Shenzhen, China (II), The Hong Kong University of Science and Technology, Hong Kong, China, 2000, pp. 805–814.
[14] K. Wang, M.S. Konsta-Gdoutos, S.P. Shah, Hydration, rheology and strength of opc–ckd–slag binders, ACI Mater. J. 99 (2) (2002) 1–7.
[15] ACI 233R-95, Ground granulated blast furnace slag as a cementitious constituent in concrete, American Concrete Institute, 1995.
[16] M.S. Konsta-Gdoutos, K. Wang, P.M. Babaian, S.P. Shah, Effect of cement kiln dust on the corrosion of reinforcement of concrete, in: N. Banthia, K. Sakai, O.E. Gjorv (Eds.), Third International Conference on Concrete Under Severe Conditions of Environment and Loading, University of British Columbia, Vancouver, BC, Canada, June 18–20, 2001, pp. 277–284.
[17] C. Shi, Studies on several factors affecting hydration and properties of lime pozzolan cements, J. Mater. Civ. Eng. 13 (6) (2001) 441–445.